Research Article
Hittite Journal of Science and Engineering, 2024, 11 (1) 1-6
ISSN NUMBER: 2148-4171
DOI: 10.17350/HJSE19030000325

Effect of Crusher Arm Position and Surface Friction on the Mechanical Behaviour of a Crusher under Static Conditions

Mustafa Murat Yavuz
İzmir Democracy University, Mechanical Engineering, Izmir, Türkiye

ABSTRACT

Crushers are utilized to break down or crush various components in industrial applications are subjected to high stresses. The crushing process is carried out by a crusher arm located on the crusher itself. The shape and length of the crusher arm influence the deformation on the arm and the efficiency of crushing process. During the crushing process, stress concentrations occur at the contact regions and especially at the connection location of the crusher arm and the drive shaft. This study examined the connection of the crusher arm at various positions on the shaft and explored variations in stress. Finite element analysis was used in the analyses. The used material is standard steel that behaved elastically. The stresses changed in a way that was not proportional to the movement of the tangential crusher arm towards the center of the shaft. The d=8 mm and d=24 mm locations are the most suitable places to move the crusher arm rather than the tangential position (d=40 mm). The highest stresses occurred at the corners where the shaft and crusher arm connected and formed a stress concentration. The friction effects on the contact surface were also examined and the increased friction coefficient slightly reduced the stress values of the crusher system, but increased the stresses on the crushed object. Only maximum stress levels that are observed at the surface of the beam are mainly considered. The results regarding the crusher arm are discussed in detail.

Keywords:
Crusher; Contact interaction; Deformation; Friction; Sliding distance

Article History:
Received: 2023/02/08
Accepted: 2023/12/19
Online: 2024/03/31

***Correspondence to**: Mustafa Murat Yavuz, İzmir Democracy University, Mechanical Engineering, 35140, İzmir, TÜRKİYE*
E-Mail: murat.yavuz@idu.edu.tr;
Phone: +90 232 260 1001;
Fax: +90 232 260 1004.

This article has been checked for similarity.

INTRODUCTION

Devices that have a motor and a crusher arm mechanism are called a crusher and crusher systems. They use these parts to apply a compressive force and break down objects. Due to surface-to-surface in a limited location or surface-to-point contact, high stresses occur in the crusher arm which can cause fracture. Also these stresses cause deformations in the arm and they must remain within certain limits. The crusher arm is structurally in the beam profile and bending is the most dominant condition that happens during crushing. In the literature, there are different application trials for the solution of bending beam problem. Reinforced recycled concrete beams [1] were analyzed under bending which showed lower compressive strength and modulus of elasticity than normal concrete. A function was expressed between the compressive strength of recycled concrete and Young's modulus. Wang [2] theoretically calculated the appropriate suspended roof length for a roof. Optimum placement distances of roof hanging slots were determined by considering the weight of the beam. The most suitable cell profile against impact [3] was investigated in different cell structures formed in square tubes. A bending moment occurred due to the inclined plane having different angles used in impact. The energy absorption of a steel plate system [4] was investigated using the finite element method and it was found that most of the absorbed energy was bending energy. In a study transverse ice breaking under crushing and bending conditions, results of force/moment [5] were given. The crush response of two nested rectangular pipes under lateral compression [6-8] was investigated. Crushing load varied according to the area occupied by the plastic zone, tube thickness and yield stress of the material. Zhang et al. [9] investigated rectangular tubing which was fabricated by bending of aluminum sheets under axial crushing. The overlapping plates used in the

Cite as:
Yavuz MM. Effect of Crusher Arm Position and Surface Friction on The Mechanical Behaviour of a Crusher Under Static Conditions. Hittite Journal of Science and Engineering 2024; 11(1):1-6. doi:10.17350/hjse19030000325

tube increased the absorbed energy but caused uneven buckling. The clamped boundary condition solved that problem. Crushing behavior of CF/EP composites [10] were analyzed under quasi-static and dynamic conditions. In the quasi-static analysis, bending, an important factor of the damage mechanism, was found dominant. The average crushing force of multistage nested rectangular tubes [11] was analyzed, and the use of more stages resulted in better crush performance and energy absorption. When the number of stages or cells used [12] was increased, the crash-resistance properties were improved. Energy absorption and crushing performance of capped cylindrical tubes [13] were analyzed under oblique impact which showed better energy absorption performance than standard cylindrical tubes. The samples containing concrete and timber in the steel column tubes were tested for their stability under crushing [14]. The location of loading affected material loading capacity. An axial compression load [15] was applied to corrugated tubes containing carbon fiber reinforced polymer (CFRP) and Kevlar fiber-reinforced polymer (KFRP) composites and having conical angles of 35^0, 40^0, 45^0, 50^0 and 55^0. Similar crushing behavior was observed between KFRP and CFRP composites and 50^0 conical angle has the best energy absorption behavior. The mechanical behavior of the lattice cylindrical shells under compression [16] was investigated and negative Poisson ratio was observed. Energy absorption capacity was increased 20% between 4 different trials. Transverse bending of thin-walled beams [17] was analyzed without considering various shapes/dimensions and fixed boundary conditions. The used three-point bending analysis results showed that loading angle and position affect the deformation modes. In studies carried out on crushers that have a conical structure rather than a beam structure, heat treatment [18] was applied on a cone crusher surface to increase the resistance to abrasion. Gyratory crusher torque analysis [19] was analyzed with discrete element method and found that large particles cause to decrease the crushing torque. Another study [20] analyzed the concave curve height, curve radius, and shaft speed of a gyratory crusher to optimize its geometrical parameters. Frequency [21] for a vibratory crusher, rotor parameters [22] for a crusher-shredder, hammers, and knives [23] on rotor for crushing were investigated. Rotor parameters and hammer shape were found to be the most important design criteria. Discrete element method [24] was used to examine new hammer designs for laboratory-scale jaw crusher and new designs have been found less effective than existing designs. Thus, time/money savings were achieved by not producing industrial sized devices. Investigating single and double rotor impact crushers through the discrete element method [25] revealed that enhancing crushing efficiency is achieved by employing double rotors and elevating the rotation speed of the rotor. A general used model for crushing process has not been developed, Mishchuk et al. [26] investigated for five different crushing machines by considering destruction energy of materials. They detected that many tries into the mathematical modeling of material fracture have faced considerable challenges. The review of literature highlighted a deficiency in relevant research concerning a beam constructed on the drive shaft.

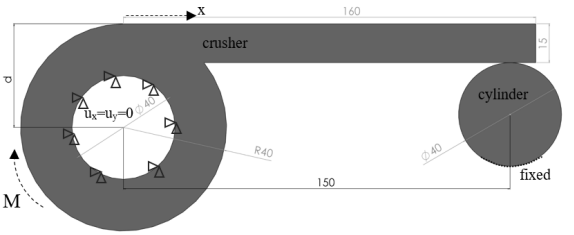

Figure 1. Geometrical model of crusher and cylinder and dimensions (in mm).

In this study, the position of the crusher arm on the shaft body and the surface friction coefficient were examined, stress and deformations were given. The study may contribute to the same or beam-shaft connection studies in the literature.

MATERIAL AND METHODS

The crusher system consists of a crusher arm and the part to be crushed and are shown in Fig. 1. The arm that crushes the material is made of beam is connected to a hollow shaft. The inner part of the shaft is defined as the cylindrical boundary condition that allows only rotational. The boundary condition defined for the rotation of the shaft around a fixed axis is also used in similar studies in the literature [27]. A torque of 1000 Nm is applied to the shaft in a clockwise direction. The piece to be broken has a circular geometry and is mounted in contact with the crusher arm. The bottom surface of the circular piece is fixed. The fixing location is sufficiently far from the contact location. Contact surfaces were defined as friction surfaces and the friction coefficient was determined as 0.3. The position of crusher arm is defined as d is shown in Fig. 1. It is the distance between the outer surface of the crusher arm and the center of the shaft. Different d values have been investigated in the study.

Finite element model of the crusher system was shown in Fig. 2 which was created to include uniform finite element distribution. There are approximately 30,000 finite elements in each model. The aspect ratio of the elements is very close to 1 and high-quality element structure is formed. The model was created with the plane stress condition in 2D with unit thickness. Standard steel (E=200 GPa, υ=0.3) was chosen as the material.

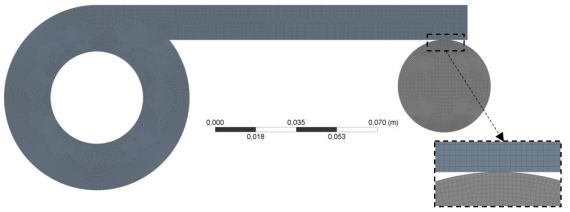

Figure 2. Finite element model of crusher and cylinder.

Figure 3. Finite element model of a cantilever beam.

A validation study was conducted to determine the solution precision and accuracy of the finite element model. Since the bending behaviour is dominant, a cantilever beam problem has been investigated and its model is shown in Fig. 3. One of the short sides of the cantilever beam is fixed and a pure moment of 10 Nm is applied to the other free edge. Cantilever beam has a length of 100 mm and height of 10 mm. The bending stress was [28] given in Eq. 1 for this validation case. The applied moment is represented as M, the distance between the geometric center and the upper/lower surface is represented as c and the moment of inertia is represented as I for the rectangular section.

$$\sigma = \frac{M \times c}{I} \tag{1}$$

The stresses in the crusher are given in the form of Von-Mises stresses [28-29] in Eq. 2. The stresses on the right side of the equation are the principal stresses.

$$\sigma_{VM} = \sqrt{\sigma_1^2 - \sigma_1\sigma_2 + \sigma_2^2} \tag{2}$$

RESULTS AND DISCUSSION

The analytical solution of validation case is given in Eq. 3. and the result obtained for the finite element analysis is shown in Fig. 4. The calculated analytical result and the results obtained from the finite element analysis are consistent with each other. The crusher system was modelled and examined using this element structure.

$$\sigma = \frac{M \cdot c}{I} = \frac{10\text{Nm} \cdot 0.005\text{m}}{\frac{1}{12} \times 1 \times (0.01\text{m})^3} = \pm 0.6\text{MPa} \tag{3}$$

In Fig. 5, the maximum Von-Mises stresses in the crusher system with respect to crusher arm distance (d) are

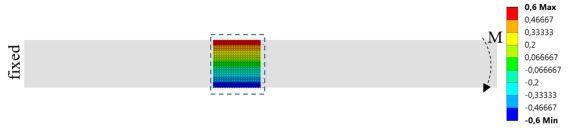

Figure 4. Bending stress of cantilever beam (in MPa).

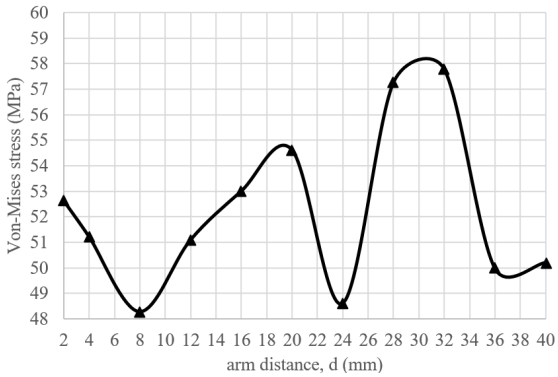

Figure 5. Crusher arm distance (d) and stresses in the system (MPa).

shown. At the farthest distance (d=40 mm) where the breaker arm is tangential to the shaft, the stress value is 50,198 MPa. Stress concentration occurs locally at the corner of the breaker arm and shaft connection. When the crusher arm was brought a little closer to the shaft center (from d=40 mm to d=36 mm), the stress value decreased slightly. As the arm that breaks the material approached the center of the hollow shaft, the connection location where the shaft and the arm meet became less acute. Stress values increased by 15% between d=36 mm and d=32 mm results. In this layout, the center of the cylindrical part and the center of the shaft are in approximately the same vertical position. The highest stress value is observed in the result with d=32 mm. There is a sharp stress reduction observed at d=24 mm results. Sharp corners turned into two normal connection corners. The lowest stress value was obtained at d=8 mm and then at d=24 mm. Geometric nonlinearity is quite dominant in stress values.

Considering the stress contours in Fig. 6, the highest stresses occurred at the corners where the crusher arm and the shaft are connected, and on the upper and lower surfaces of the crusher arm. The stress contour values are labeled as H++, H+, H, L and L- from highest to lowest. The highest stress (H++) locations occur at the connection corners in all cases. When the crusher arm is approaching to the centre of shaft (from d=40 mm to d=32 mm), H+ stress location vanishes at the upper surface of the crusher arm. H+ location at the below surface of the crusher arm concentrates in a smaller area. Therefore, the stress value at d=32 mm is higher than the other cases. H+ contours appear at the upper surface of the crusher arm in d=24 mm results that causes to decrease the stresses at the lower surface. At the d=2 mm result, two H++ stress locations are observed. This stress distribution is similar the stress distribution of a cantilever beam under bending.

The stresses occurring on the upper surface of the crusher arm are shown in Fig. 7. Stress concentration have occurred at the x=0 m location, where the crusher arm connects with the shaft. In the results of d=40 mm, stress values

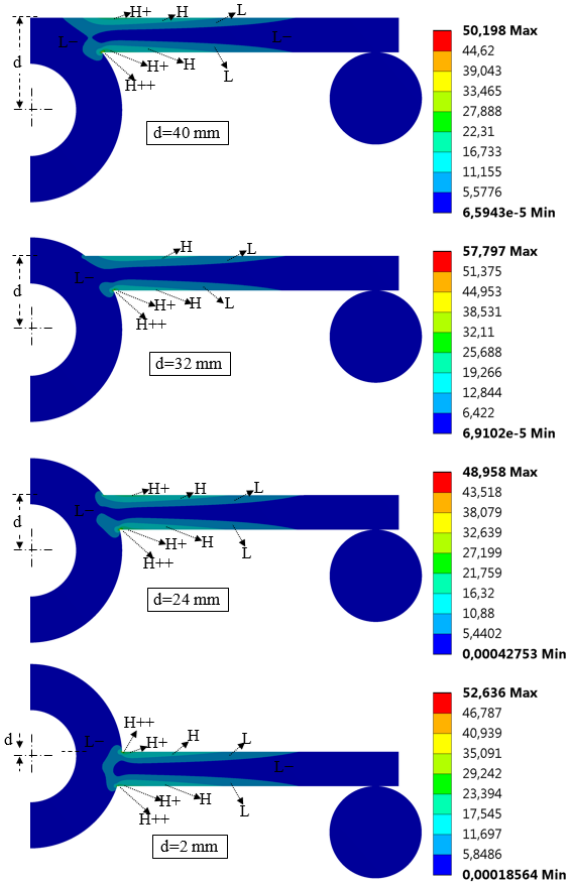

Figure 6. Von-Mises stress (in MPa) contours for d=40, 32, 24 and 2 mm.

are not high at x=0 m. This is caused by the fact that the crusher arm of the d=40 mm model is completely tangential to the shaft outer surface. There is no formation of a protrusion at the x=0 m. As a result of the decrease in the d distance of the crusher arm, the crusher arm approach towards the center of the shaft created a protrusion on the connection location between the shaft and the upper surface of the crusher arm. A stress concentration occurs at x=0 m with the effect of protrusion. The highest stresses after x=0 m range from 18 to 19 MPa. The stress value decreased as the d value decreased.

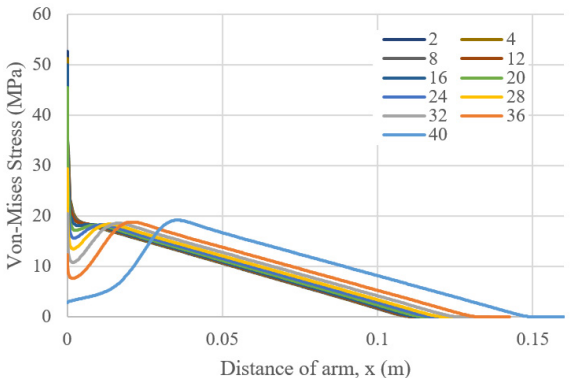

Figure 7. Von-Mises stresses on the upper surface of the crusher arm at different d distance.

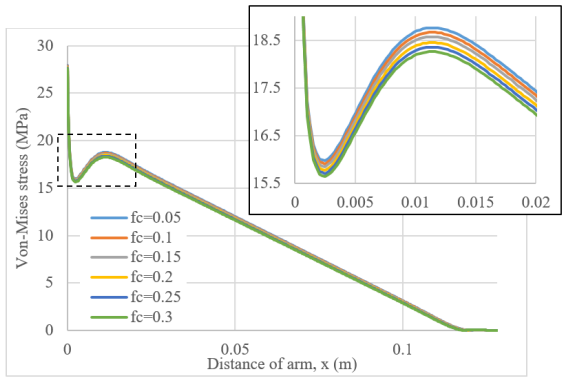

Figure 8. Effect of fc on Von-Mises stresses of d=24 mm model at upper surface.

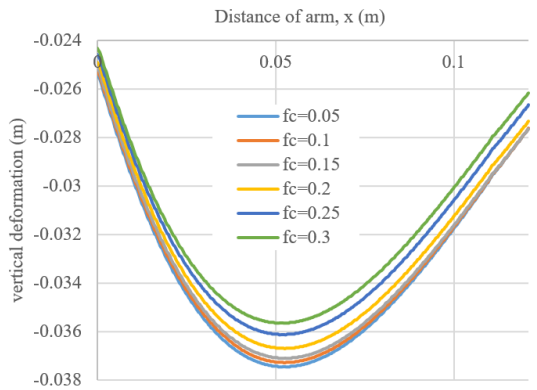

Figure 9. Vertical deflection results on the lower surface of the crusher arm for the d=24 mm model.

In Fig. 8, the effect of friction coefficient (fc) is shown for the d=24 mm crusher arm model. The results are taken from upper surface of the crusher arm. It has been observed that increasing friction coefficient reduces stresses. A magnified view is also added at the protrusion location. Increasing the fc from 0.05 to 0.3 decreased the stresses by 2.6%. The stress distribution does not change much as different fc values. The effect of fc on the vertical deflection results are shown in Fig. 9 for the d=24 mm model. The highest deflection occurred in the middle of the crusher arm. Deflection results are reduced when the friction coefficient (fc) increases.

The stress and support reactions are shown in Table 1 at different coefficients of friction for the d=24 mm model. The reaction forces (fx, fy) that occur where the crushed part is fixed are shown. Same magnitudes of these reaction forces occur at the cylindrical boundary conditions of the shaft, but opposite direction. The reaction moment acts to prevent the rotation of the object that is being crushed. As the friction coefficient increased, the horizontal force and the stress values on the cylinder increased, and this had a positive effect on the crushing situation. The stress in the crusher decreased with increasing friction coefficient.

Table 1. Stress and reaction responses for d=24 mm model.

fc	stress in system (MPa)	stress in cylinder (MPa)	force rea. Fx (N)	force rea. Fy (N)	moment rea. Ma (Nm)
c	50.5	4.69	-312.28	6649.0	11.89
0.1	50.1	4.74	-621.27	6630.4	23.76
0.15	49.8	4.81	-928.47	6612.0	35.55
0.2	49.3	4.95	-1320.6	6588.4	50.60
0.25	49.0	5.13	-1643.6	6569.0	63.00
0.3	48.6	5.33	-1966.3	6549.6	75.38

CONCLUSION

This study examined how the location of the arm and the coefficient of friction on the surface affected a system that crushes materials. Finite element method was used, and stresses, deflection and reaction forces formed under the effect of constant moment were given. In the results obtained;

- Due to the moment applied to the breaker, mainly bending stress has occurred in the breaker arm.
- Sharp corners at the connection locations of the crusher arm and shaft has the highest stress locations.
- The absence of sharp corner on the upper surface of the crusher arm caused the least stress formation at the upper surface (in d=40 mm case)
- Moving the tangentially crusher arm (d=40 mm) towards the d=8 mm and d=24 mm locations reduces the stresses.
- Increasing the friction coefficient increases the horizontal reaction force and the stress in the crushed part while decreases the total stress value of the crusher system and vertical deflection of the crusher arm.

CONFLICT OF INTEREST

The author declares no conflict of interest.

References

1. Sato R, Maruyama I, Sogabe T, Sogo M. Flexural behavior of reinforced recycled concrete beams. Journal of Advanced Concrete Technology. 2007;5(1):43-61.
2. Wang K. Study of reasonable hanging roof length on hard roof. Procedia Engineering. 2011;26:772–77.
3. Tran T, Hou S, Han X, Nguyen T, Chau M. Theoretical prediction and crashworthiness optimization of multi-cell square tubes under oblique impact loading. International Journal of Mechanical Sciences. 2014;89:177–193.
4. Dong H, Gao G, Chen X, Guan W, Zou X. Crushing analysis of splitting–bending steel plate energy absorber under axial loading. International Journal of Mechanical Sciences. 2016;110:217–228.
5. Zhou L, Riska K, Ji C. Simulating transverse icebreaking process considering both crushing and bending failures. Marine Structures. 2017;54:167-87.
6. Tran T. A study on nested two-tube structures subjected to lateral crushing. Thin-Walled Structures. 2018;129:418–28.
7. Mohsenizadeh S, Ahmad Z. Auxeticity effect on crushing characteristics of auxetic foam-filled square tubes under axial loading. Thin-Walled Structures. 2019;145(106379):1-21.
8. Li J, Gao G, Yu Y, Guan W. Experimental and numerical study on splitting process of circular steel tube with enhanced crashworthiness performance. Thin-Walled Structures. 2019;145(106406):1-11.
9. Zhang X, Zhang H, Ren W. Axial crushing of tubes fabricated by metal sheet bending. Thin-Walled Structures. 2018;122:252–263.
10. Chen Y, Ye L, Escobedo-Diaz JP, Zhang Y, Fu K. Quasi-static and dynamic progressive crushing of CF/EP composite sandwich panels under in-plane localised compressive loads. Composite Structures. 2019;222(110839):1-11.
11. Tran T, Le D, Baroutaji A. Theoretical and numerical crush analysis of multi-stage nested aluminium alloy tubular structures under axial impact loading. Engineering Structures. 2019;182:39–50.
12. Wu Y, Fang J, Cheng Z, He Y, Li W. Crashworthiness of tailored-property multi-cell tubular structures under axial crushing and lateral bending. Thin–Walled Structures. 2020;149(106640):1-22.
13. Reddy KY, Kumar AP, Nagarjun J. A computational study on the crushing behaviour of aluminium capped cylindrical tubes subjected to oblique load. Materials Today: Proceedings. 2020;27:1923–27.
14. Ghanbari-Ghazijahani T, Nabati A, Azandariani MG, Fanaie N. Crushing of steel tubes with different infills under partial axial loading. Thin–Walled Structures 2020;149(106614):1-14.
15. Alkhatib F, Mahdi E, Dean A. Crushing response of CFRP and KFRP composite corrugated tubes to quasistatic slipping axial loading: Experimental investigation and numerical simulation. Composite Structures. 2020;246(112370):1-16.
16. Guo Y, Zhang J, Chen L, Du B, Liu H, Chen L, Li W, Liu, Y. Deformation behaviors and energy absorption of auxetic lattice cylindrical structures under axial crushing load. Aerospace Science and Technology. 2020;98(105662):1-11.
17. Huang Z, Zhang X, Fu X. On the bending force response of thin-walled beams under transverse loading. Thin–Walled Structures. 2020;154(106807):1-10.

18. Allende-Seco R, Artigas A, Bruna H, Carvajal L, Monsalve A, Sklate-Boja MF. Hardening by transformation and cold working in a hadfield steel cone crusher liner. Metals. 2021;11(6):961.
19. Moncada M, Toledo P, Betancourt F, Rodríguez CG. Torque analysis of a gyratory crusher with discrete element method. Minerals. 2021;11(8):878.
20. Chen Z, Wang G, Xue D, Cui D. Simulation and optimization of crushing chamber of gyratory crusher based on the DEM and GA. Powder Technology. 2021;384:36–50.
21. Mishchuk YO, Nazarenko II, Mishchuk DO, Definition of rational operating modes of a vibratory jaw crusher. Naukovyi Visnyk Natsionalnoho Hirnychoho Universytetu. 2021;4:56-62.
22. Astanakulov K, Karshiev F, Gapparov S, Khudaynazarov D, Azizov S, Mini crusher-shredder for farms. E3S Web of Conferences, Conmechydro. 2021;264(04038):1-8.
23. Tamborrino A, Perone C, Veneziani G, Berardi A, Romaniello R, Servili M, Leone A. Experimental investigation of a new modular crusher machine developed for olive oil extraction plants. Foods. 2022;11:3035.
24. Doroszuk B, Król R. Industry Scale optimization: hammer crusher and dem simulations. Minerals. 2022;12:244.
25. Bwalya MM, Chimwani N. Numerical simulation of a single and double-rotor impact crusher using discrete element method. Minerals. 2022;12:143.
26. Mishchuk YO, Nazarenko II. Analysis of the energy laws of material destruction. Strength of Materials and Theory of Structures. 2023;110:294-315
27. Trahair NS. Non-linear biaxial bending of steel Z-beams. Thin-Walled Structures. 2018;129:317–26.
28. Budynas R, Nisbett K. Shigley's mechanical engineering design 11th Edition, McGraw Hill; 2020.
29. Young WC, Budynas RG. Roark's formulas for stress and strain, Seventh Edition, McGraw-Hill; 2002.